N91-17082

IONOSPHERIC REFRACTION EFFECTS ON ORBIT DETERMINATION USING THE ORBIT DETERMINATION ERROR ANALYSIS SYSTEM*

C. P. Yee, D. A. Kelbel, T. Lee, and J. B. Dunham
COMPUTER SCIENCES CORPORATION

G. D. Mistretta
GODDARD SPACE FLIGHT CENTER

ABSTRACT

The influence of ionospheric refraction on orbit determination has been studied through the use of the Orbit Determination Error Analysis System (ODEAS). This paper presents the results of a study of the orbital state estimate errors due to the ionospheric refraction corrections, particularly for measurements involving spacecraft-to-spacecraft tracking links.

In current operational practice at the Goddard Space Flight Center (GSFC) Flight Dynamics Facility (FDF), the ionospheric refraction effects on the tracking measurements are modeled in the Goddard Trajectory Determination System (GTDS) using the Bent ionospheric model. While GTDS has the capability of incorporating the ionospheric refraction effects for measurements involving ground-to-spacecraft tracking links, such as those generated by the Ground Spaceflight Tracking and Data Network (GSTDN), it does not have the capability to incorporate the refraction effects for spacecraft-to-spacecraft tracking links for measurements generated by the Tracking and Data Relay Satellite System (TDRSS). The lack of this particular capability in GTDS raised some concern about the achievable accuracy of the estimated orbit for certain classes of spacecraft missions that require high-precision orbits. Using an enhanced research version of GTDS, some efforts have already been made to assess the importance of the spacecraft-to-spacecraft ionospheric refraction corrections in an orbit determination process. While these studies were performed using simulated data or real tracking data in definitive orbit determination modes, the study results presented in this paper were obtained by means of covariance analysis simulating the weighted least-squares method used in orbit determination.

The current operational version of ODEAS has the capability to compute ionospheric refraction corrections for range and range-rate measurements for both GSTDN and TDRSS data using the Bent ionospheric model. Using this capability in ODEAS, this study demonstrates how the magnitude and the characteristics of the spacecraft-to-spacecraft ionospheric refraction depend on such factors as spacecraft altitudes, solar activity, tracking geometry, and the local solar times of measurements. This study also provides error analysis results showing how the ionospheric refraction affects the spacecraft state estimate errors for routine orbit determination of spacecraft missions such as Gamma Ray Observatory (GRO), depending on the tracking geometries and the tracking pass lengths. ODEAS is a software system particularly convenient for analyses of this type. The results obtained from this study will provide a quick reference for ionospheric refraction effects on orbit determination and will be useful for assessing orbit accuracy requirements for many future spacecraft missions.

* This work was supported by the National Aeronautics and Space Administration (NASA)/Goddard Space Flight Center (GSFC), Greenbelt, Maryland, under Contract NAS 5-31500.

1.0 INTRODUCTION

The Earth's ionosphere extends from approximately 80 kilometers to beyond 1000 kilometers from the surface of the Earth and consists of ionized particles. As a tracking signal travels through this medium, the refraction or bending of the signal path occurs due to the presence of free electrons. The magnitude of refraction is dependent upon the electron densities along the path of the tracking signal and the frequency of the signal. To achieve high accuracy in determining a spacecraft orbit, it is therefore necessary to properly correct the tracking data for the refraction effects.

In the current operational practice at the Goddard Space Flight Center (GSFC) Flight Dynamics Facility (FDF), the ionospheric refraction effect is computed in the Goddard Trajectory Determination System (GTDS) for ground-to-spacecraft tracking links using a global electron density model known as the Bent model (References 1 and 2). However, no refraction correction is performed for spacecraft-to-spacecraft links for Tracking and Data Relay Satellite System (TDRSS) data; therefore, TDRSS tracking data are only partly corrected for ionospheric refraction. To circumvent this deficiency, a geometrical editing criterion can be employed in GTDS to reject the tracking data subject to significant ionospheric disturbance. This practice reduces the amount of tracking data actually used for the orbit determination process. It is therefore desirable to know the characteristics and the magnitude of the ionospheric refraction corrections and how they influence the accuracy of orbit determination. Such information will be useful to an orbit analyst in assessing the accuracy requirements of the spacecraft missions and will provide insights into ways of achieving more accurate spacecraft orbits by minimizing the orbit errors associated with the ionospheric refraction corrections. Using an enhanced research version of GTDS, some efforts have already been made to assess the importance of the spacecraft-to-spacecraft ionospheric refraction corrections in an orbit determination process (Reference 3). While these studies were performed using simulated data or real tracking data in definitive orbit determination modes, the study results presented in this paper were obtained by means of covariance analysis simulating the weighted least-squares method used in orbit determination.

This paper presents results obtained by using the Orbit Determination Error Analysis System (ODEAS). ODEAS is a general-purpose linear orbit determination error analysis system which can be used as a covariance analysis tool to analyze the orbit determination errors resulting from various systematic error sources and random noises. Throughout the study, the Earth's ionosphere was modeled as a nonhomogeneous medium based upon the Bent model. The study results can be divided into two parts. The first part presents the magnitude and the general characteristics of ionospheric refraction correction as a function of spacecraft-to-spacecraft tracking geometry, solar activity, orbit inclination, user spacecraft orbital height, and local times of TDRS and the user spacecraft at the time of measurement. The second part investigates the spacecraft orbit determination errors that can result from neglecting the ionospheric refraction effects in spacecraft-to-spacecraft links. Due to the linearity assumptions involved in the orbit estimation process, the results obtained can also be extended to address the effects of inexact modeling of ionospheric refraction in spacecraft-to-spacecraft tracking links by simple linear scaling. The results for a spacecraft mission such as the Gamma Ray Observatory (GRO) are discussed.

A brief background of the Bent model is provided in Section 1.1 of this paper. Section 1.2 describes the mathematical procedures used in ODEAS for modeling the ionospheric refraction correction for spacecraft-to-spacecraft links using the Bent model. Section 2 discusses the study results, and Section 3 presents conclusions and recommendations.

1.1 BENT MODEL

The Bent model is an empirical world-wide electron density model named after its original developers R. B. Bent et al. (Reference 2). This model was derived in the early 1970s from analysis of the many thousands of satellite and ground-based ionospheric soundings and satellite electron density measurements available at the time. It was extensively evaluated before incorporation into GTDS (Reference 4). The model provides the electron density profiles (electron density as a function of altitude) derived by incorporating the effects of variations in latitude, longitude, solar activity, geomagnetic activity, seasonal variations, and local time. Using this model, an electron density profile similar to that shown in Figure 1 can be constructed for any geographic location around the globe. This profile is represented in the Bent model using seven curve sections, including two parabolic sections and five exponential tail sections.

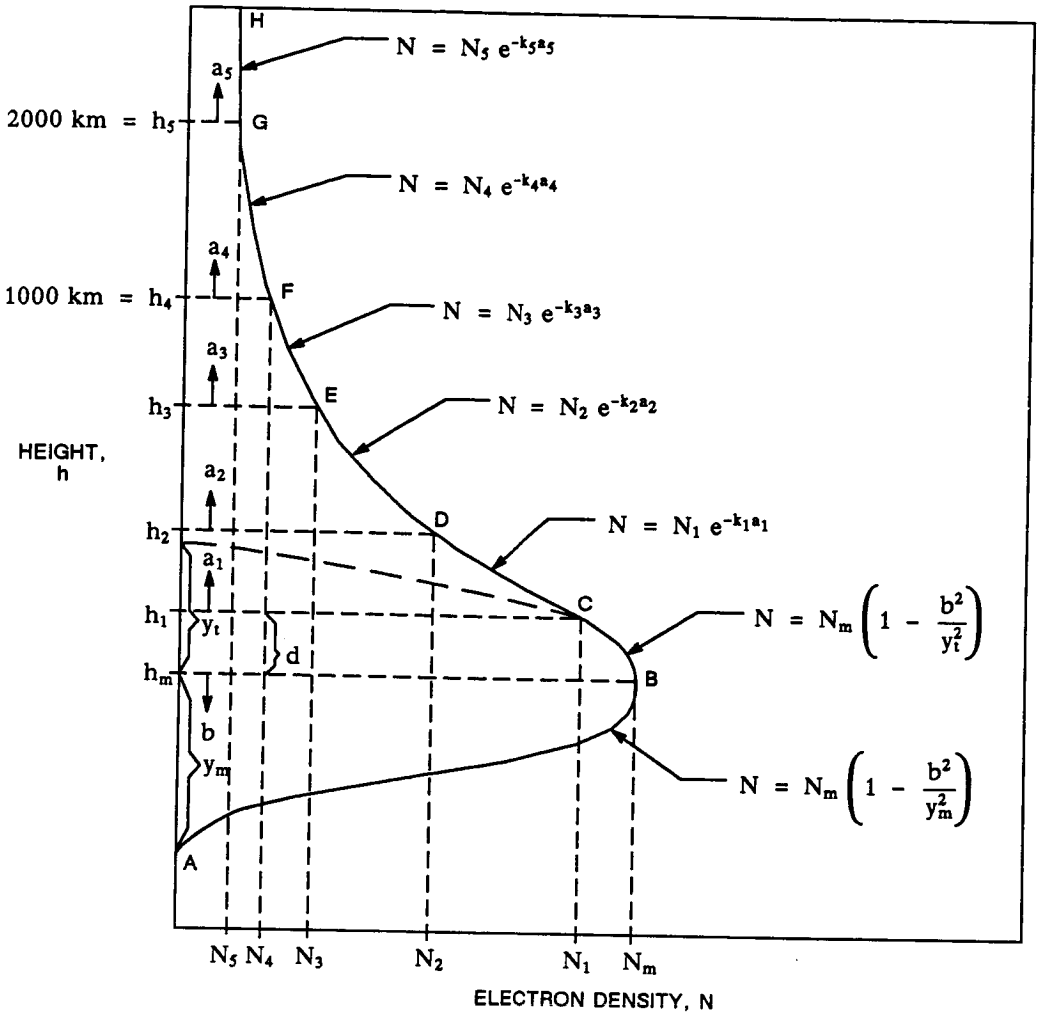

Figure 1. Empirical Worldwide Electron Density Profile

The computation of the electron density profile consists of evaluating parameters specifying the upper and lower parts of the parabolic section including the maximum density, N_m, the corresponding altitude, h_m, and the exponential constants specifying the five exponential tail sections. This model has been successfully used in GTDS for correcting the ground-to-spacecraft tracking links for ionospheric refraction. The detailed mathematical description of the model as implemented in GTDS is described in Reference 1. Although the model has been successful in correcting the ground-to-spacecraft tracking measurements, the validity of the model for correcting spacecraft-to-spacecraft measurements, especially for high-altitude regions, has yet to be thoroughly evaluated for application in GTDS.

The following section discusses the ionospheric refraction corrections using the Bent model for the spacecraft-to-spacecraft links as implemented in ODEAS. Reference 5 provides the mathematical details of the model implementation.

1.2 IONOSPHERIC REFRACTION CORRECTION FOR SPACECRAFT-TO-SPACECRAFT LINKS

The ionospheric refraction effects can be characterized in terms of the variable local index of refraction, n, of the medium through which the signal is propagated. This index of refraction can be expressed as

$$n = 1 - N_I \qquad (1)$$

where N_I is the refractivity and is given in terms of the electron density, N (electrons per cubic meter), and the signal transmission frequency, f (hertz), as follows:

$$N_I = 40.3 \frac{N}{f^2} \tag{2}$$

For a given measurement, the signal frequency, f, is a constant, and the electron density, N, varies with the altitude, longitude, latitude, and local time of the signal path. The range correction due to ionospheric refraction, $\Delta\varrho_I$, can be computed by integrating N_I as expressed in Equation (2) along the signal path, as follows:

$$\Delta\varrho_I = \frac{40.3}{f^2} \int N \, ds \tag{3}$$

where ds denotes an infinitesimal ray path length.

For a spacecraft-to-spacecraft tracking link, the integral expressed in Equation (3) must be evaluated by a numerical method, because the electron density, N, cannot easily be expressed as a function of the ray path, s. In ODEAS, this integral is evaluated using a 12-point Gaussian quadrature scheme.

Figure 2 illustrates the two tracking configurations for a spacecraft-to-spacecraft tracking link that are relevant for the effects of ionospheric refraction. For configuration 1, ($\beta > 90$ degrees), the integral of Equation (3) is evaluated from the user spacecraft at U to the maximum ionospheric height at Q, which is set at 3000 kilometers. For configuration 2, ($\beta < 90$ degrees), the integral is evaluated in two parts divided at point P, the point of lowest approach for the signal path. One integration is done from point P to Q and the other from point P to U.

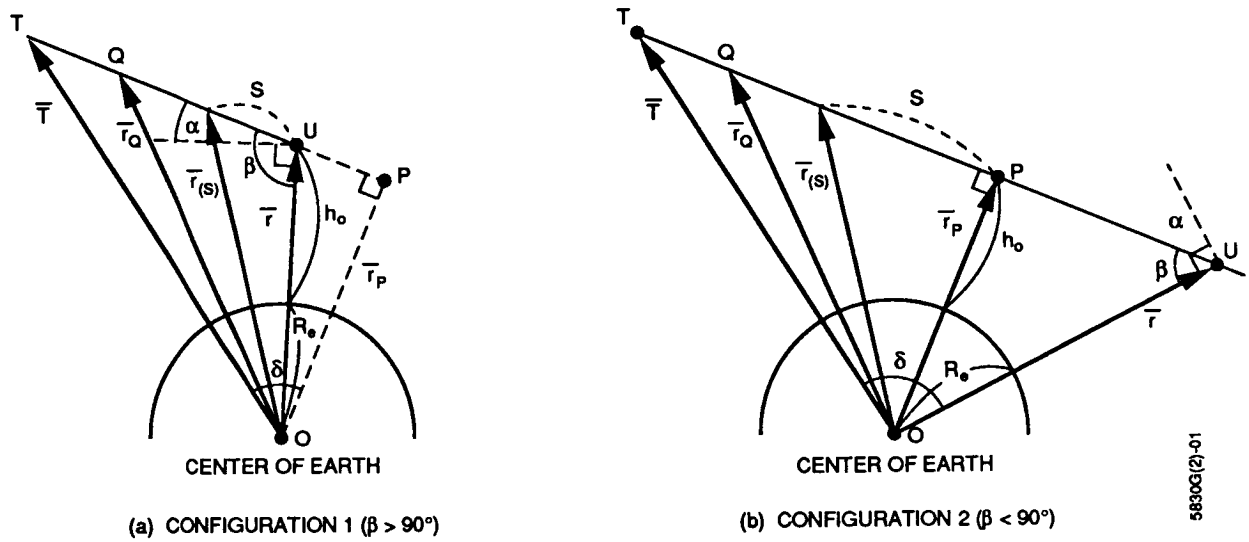

Figure 2. Spacecraft-to-Spacecraft Segment (Two Possible Configurations Shown)

In the ODEAS implementation, to achieve computational efficiency, a new electron density profile may not always be recomputed at each integration point along the ray path. A new electron density profile is computed for point s_i whenever the geographic longitude and latitude of this point are different from those of the previous integration point on the ray path, s_{i-1}, by more than a specified tolerance, i.e.,

$$|\phi_i - \phi_{i-1}| + |\lambda_i - \lambda_{i-1}| \geq \text{Tol} \tag{4}$$

where

(ϕ_i, λ_i) and $(\phi_{i-1}, \lambda_{i-1})$ = geographic latitude and longitude pairs for the points s_i and s_{i-1}, respectively

Tol = user-specified tolerance level

Therefore, by adjusting the tolerance level, the number of electron density profiles computed in the integration can be controlled. Throughout the study, the tolerance level for recomputing the electron density profile was set to 1 degree. This setting ensures recomputation of electron density profiles at each integration point along the ray path for most of the tracking geometries except for those where the integration points are very close to each other, such as in the case of large β angles, in which case the range ionospheric corrections obtained by setting Tol = 1 degree and Tol = 0.001 degree differed by less than 2 percent.

Range-rate corrections can be computed from range corrections as follows:

$$\Delta\dot{\varrho}_I = - \frac{\Delta\varrho_I(t_i) - \Delta\varrho_I(t_{i-1})}{\Delta t} \tag{5}$$

where

$\Delta\varrho_I(t_i)$ and $\Delta\varrho_I(t_{i-1})$ = two successive range corrections computed at time t_i and t_{i-1}, respectively

Δt = time difference between two measurements (usually the Doppler count interval)

2.0 RESULTS

The results of this study are presented in two parts. Section 2.1 discusses the general characteristics of ionospheric refraction correction as a function of various parameters. Section 2.2 describes the orbit determination error analysis results that can be expected by ignoring the ionospheric refraction effects in spacecraft-to-spacecraft tracking links using the routine orbit determination scenario of a GRO-type spacecraft mission as an example.

2.1 GENERAL CHARACTERISTICS OF IONOSPHERIC REFRACTION CORRECTIONS

As stated earlier, the magnitude of ionospheric refraction correction is a function of tracking signal frequency and the electron densities along the signal path as it traverses the ionosphere. This is expressed mathematically in Equation (3). For a given measurement, the frequency, f, is a constant; and the ionospheric refraction correction is complicated due to the nature of electron density representation. This section presents the magnitude and the general characteristics of ionospheric refraction correction as a function of various parameters that affect the electron densities. The parameters studied were limited to spacecraft-to-spacecraft tracking geometry, solar activity, orbital height and inclination, and local solar times of TDRS and the user spacecraft at the time of measurement. Although the ionospheric refraction can also be affected by the seasonal variation, this effect was not studied parametrically.

To study the effects of these parameters, 18 different specially designed circular orbits were investigated using ODEAS. These basic spacecraft orbits were constructed by the combination of six different orbital heights (350, 550, 750, 950, 1150, and 1350 kilometers) and three different inclinations (28.5, 63.14, and 99.03 degrees). For each basic run scenario, a 24-hour definitive period was simulated using TDRSS two-way range and range-rate tracking. The tracking signals were modeled as S-band signals, with a frequency of 2100 megahertz, and a data sampling rate of 30 seconds. As shown in Equation (3), the ionospheric refraction correction is proportional to the inverse of the signal frequency squared; and, therefore, the results obtained can be scaled appropriately for different signal frequencies. For example, the ionospheric refraction correction value obtained with a K-band signal would yield a value approximately 50 times smaller than the S-band signal.

A measurement was scheduled whenever the user spacecraft was visible to the TDRS. This was done to ensure the collection of a fairly large sample of tracking data with a variety of tracking geometries. Ionospheric refraction corrections were computed for all the spacecraft-to-spacecraft range and range-rate data. The results obtained are described below.

2.1.1 Tracking Geometry

The spacecraft-to-spacecraft tracking geometry can be characterized by the relative positions of the relay spacecraft (TDRS), the user spacecraft, and the Earth. In the TDRSS environment, the relay spacecraft is in geosynchronous orbit at a height of approximately 35,800 kilometers above the Earth's surface. Figure 2 illustrates the two tracking geometries. In Figure 2a, both the relay and the user spacecraft are on the same side of the Earth; whereas in Figure 2b, the relay and the user spacecraft are on the opposite sides of the Earth.

The elevation angle of the relay with respect to the user, α, can be defined as the line-of-sight elevation angle of the relay spacecraft as measured from the local horizontal plane at the user. This elevation angle can be computed by

$$\alpha = \beta - 90 \text{ degrees} \tag{6}$$

With this definition, the elevation angle, α, assumes a positive value in Figure 2a and a negative value in Figure 2b.

The height of ray path, h_0, is the height of a point of closest approach on the ray path. For Figure 2a, h_0 is the same as the user spacecraft orbital height. The central angle, δ, is defined as the angle between the position vectors of TDRS and the user spacecraft, subtended at the center of the Earth.

It can be seen in Figure 2 that as the elevation angle, α, decreases, there is a greater possibility that the ray path will traverse a more "diverse" ionosphere, which consists of many different electron density profiles due to bigger possibility of variations in latitude, longitude, and local times. Conversely, as the elevation angle increases, the ray path encounters the ionosphere with less diversity. Figures 3a and 3b illustrate the average ionospheric refraction for range and range-rate data as a function of elevation angle for various orbital heights at a 28.5-degree inclination. The ionospheric refraction correction value plotted at a given orbital height at a given elevation angle was obtained as an average value in the case of range correction, or as a root-mean-square (RMS) value in the case of range-rate correction, from the collection of tracking data taken at that specified elevation angle during a 24-hour period. RMS values were used for range-rate data because the ionospheric refraction corrections for range-rate data could assume positive and negative values, and the RMS can represent the mean magnitude of the correction regardless of sign.

Figures 4a, 4b and Figures 5a, 5b illustrate the same type of plots for orbital inclinations of 63.14 and 99.03 degrees. To see the spread of ionospheric refraction correction values obtained at each elevation angle, Figures 6a and 6b illustrate the maximum, minimum, and average or RMS values of the ionospheric corrections for a 28.5-degree inclination, 350-kilometer altitude orbit.

All these figures demonstrate the fact that the ionospheric refraction correction for both range and range-rate measurements decreases as the elevation angle increases. The elevation angle dependence is more pronounced for lower orbital heights (350 and 550 kilometers) and less pronounced for higher altitudes (1150 and 1350 kilometers).

Figures 3 through 5 also illustrate the functional dependence of ionospheric refraction corrections on the orbital height. It can be seen from these figures that the magnitude of corrections are generally higher for lower orbital heights. At a 350-kilometer altitude, the average ionospheric refraction corrections for range measurements are about 1.5 to 2 times as high as those values observed at a 550-kilometer altitude. As the orbital height increases, the correction values become smaller and its dependence on the orbital height become less significant. For the spacecraft orbital heights of 950, 1150, and 1350 kilometers, the corrections are found to be in the same neighborhood.

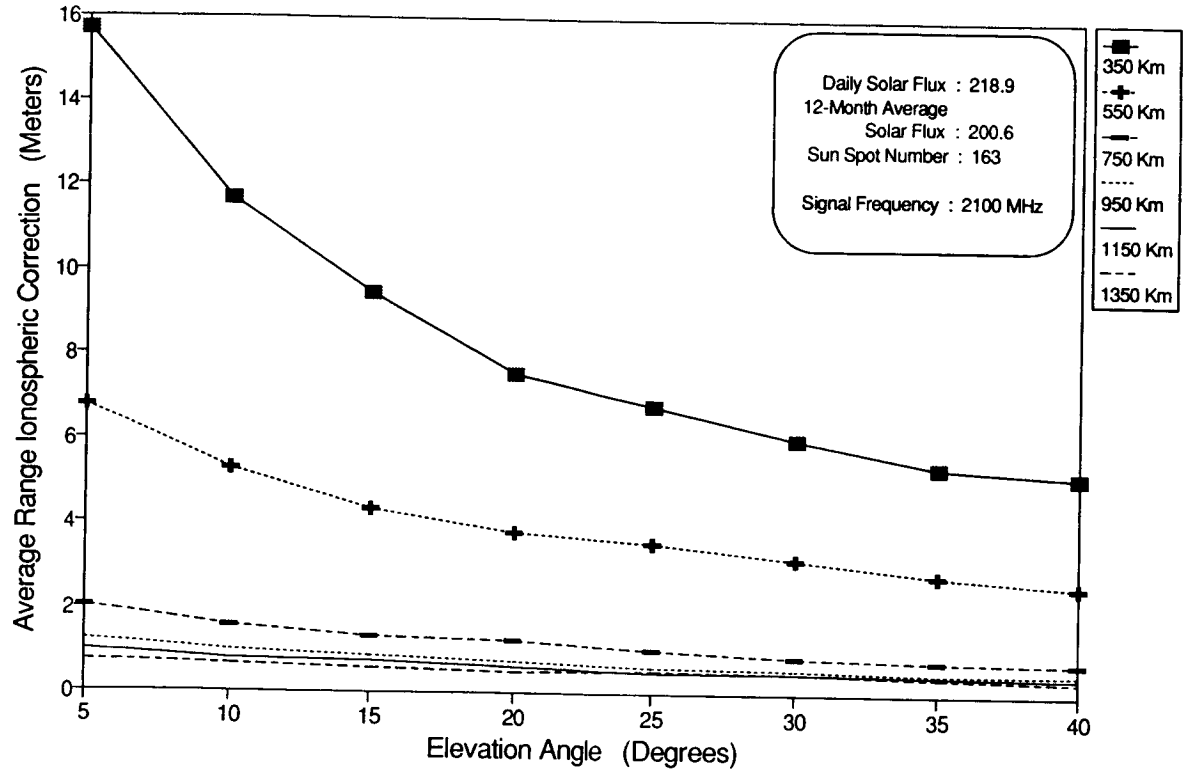

Figure 3a. Average Range Ionospheric Correction Versus Elevation Angle for a 28.5-Degree Inclination for Various Altitudes

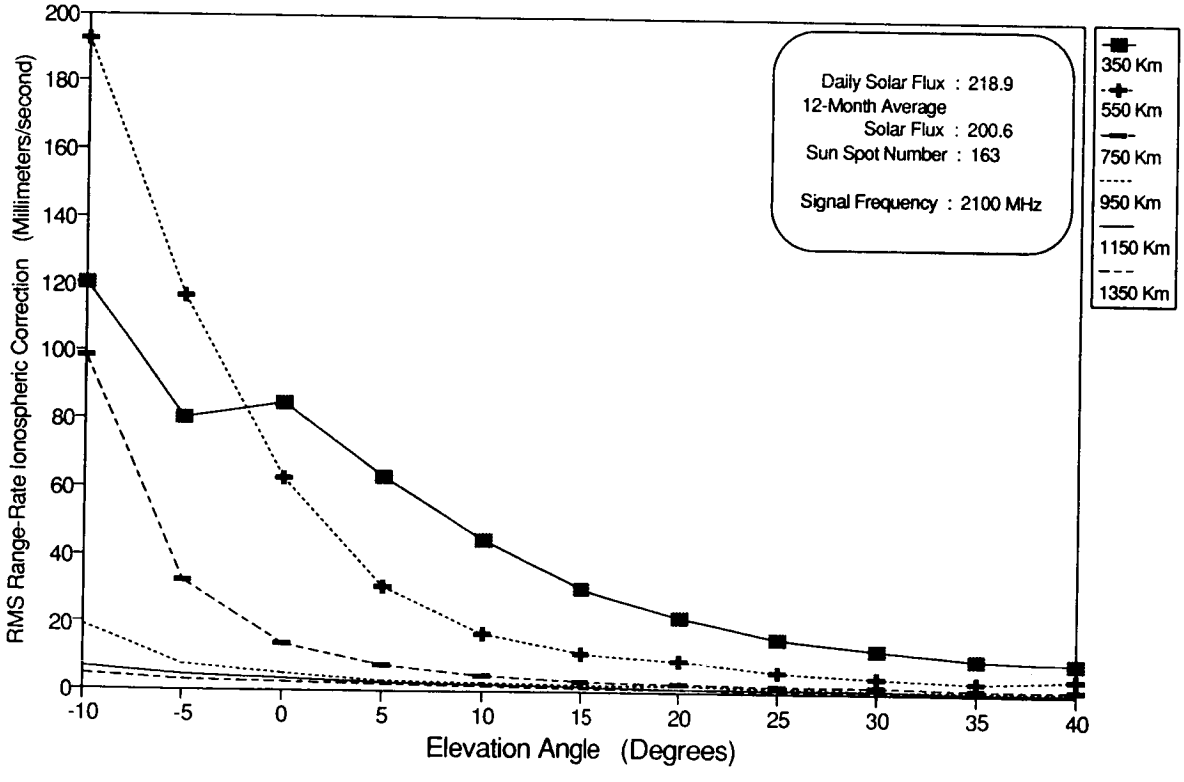

Figure 3b. RMS Range-Rate Ionospheric Correction Versus Elevation Angle for a 28.5-Degree Inclination for Various Altitudes

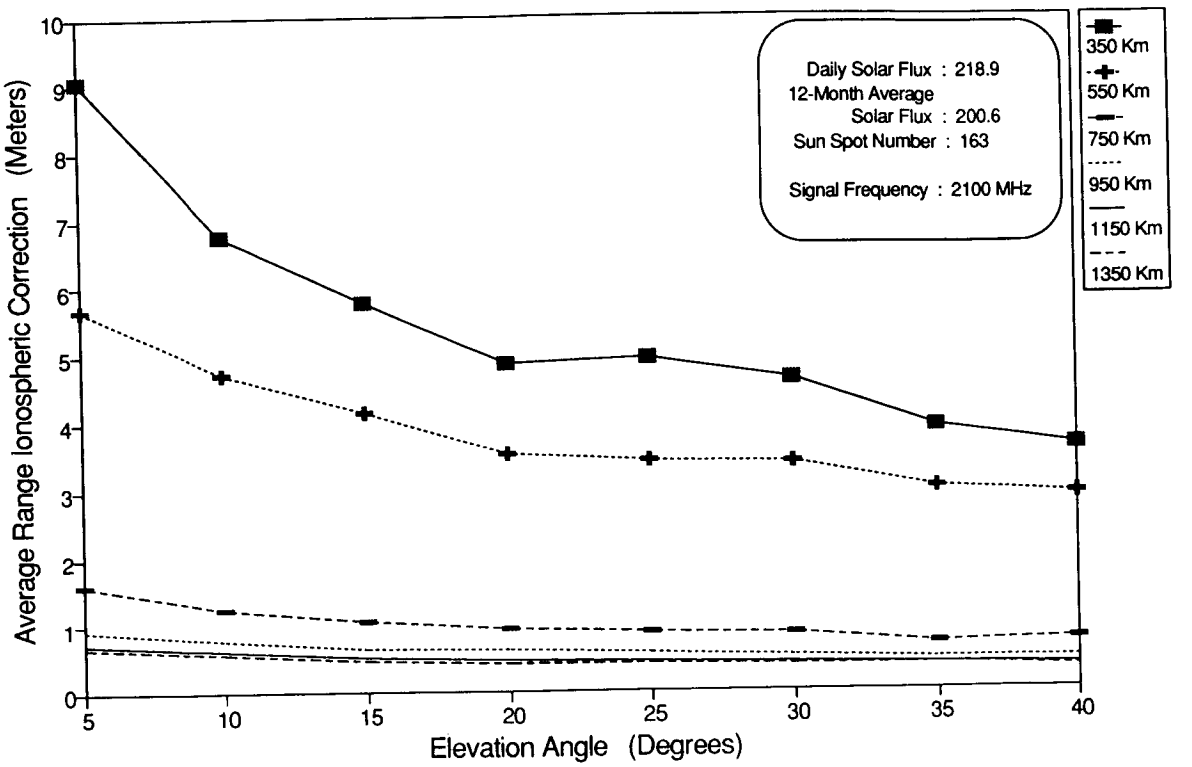

Figure 4a. Average Range Ionospheric Correction Versus Elevation Angle for a 63.14-Degree Inclination for Various Altitudes

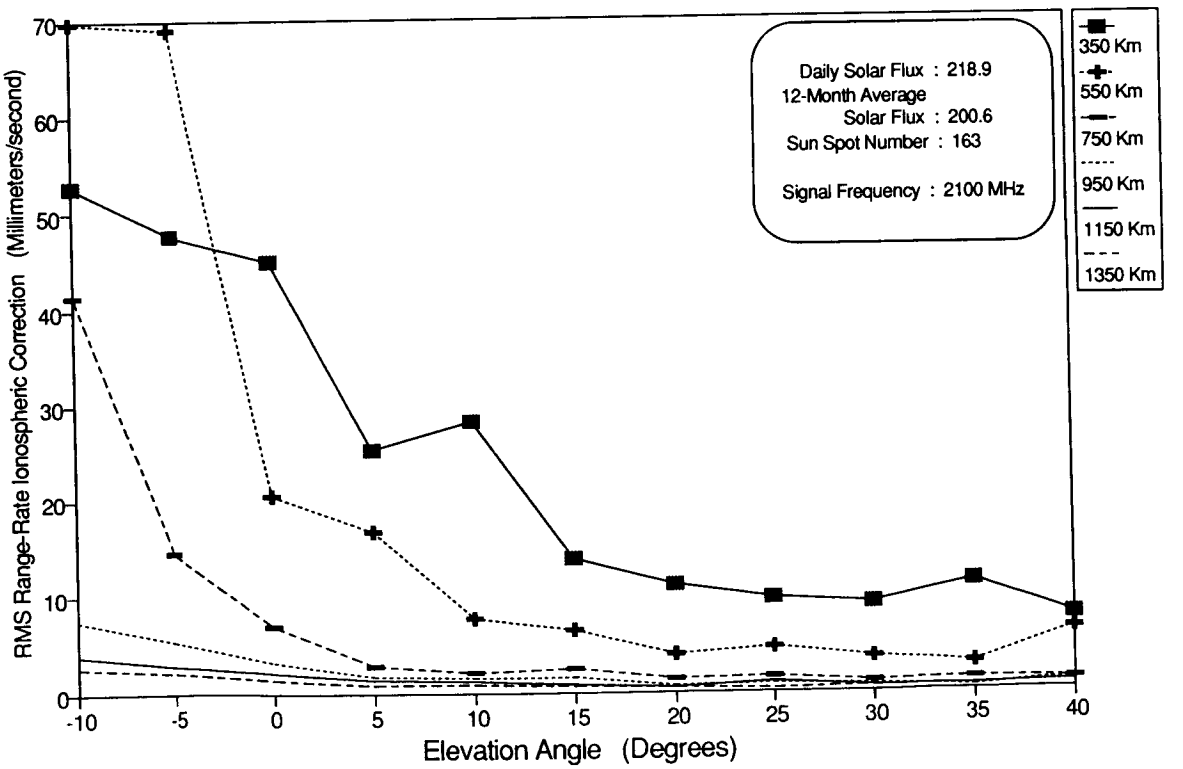

Figure 4b. RMS Range-Rate Ionospheric Correction Versus Elevation Angle for a 63.14-Degree Inclination for Various Altitudes

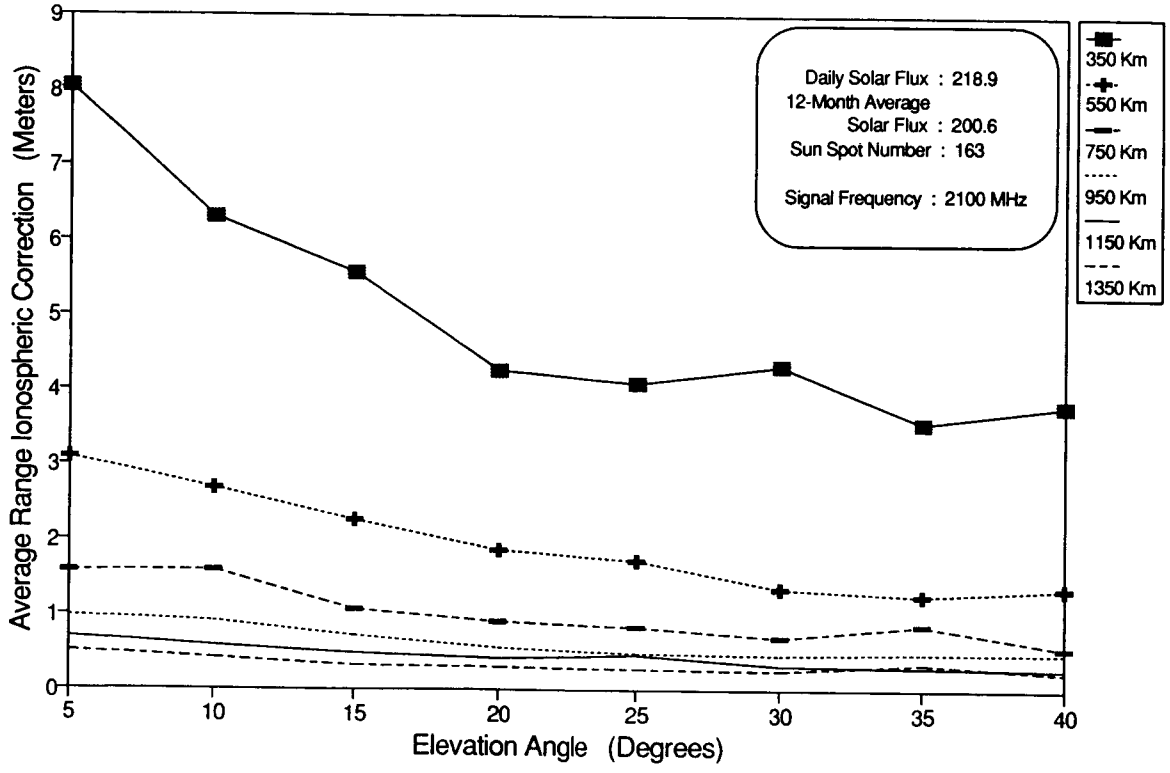

Figure 5a. Average Range Ionospheric Correction Versus Elevation Angle for a 99.03-Degree Inclination for Various Altitudes

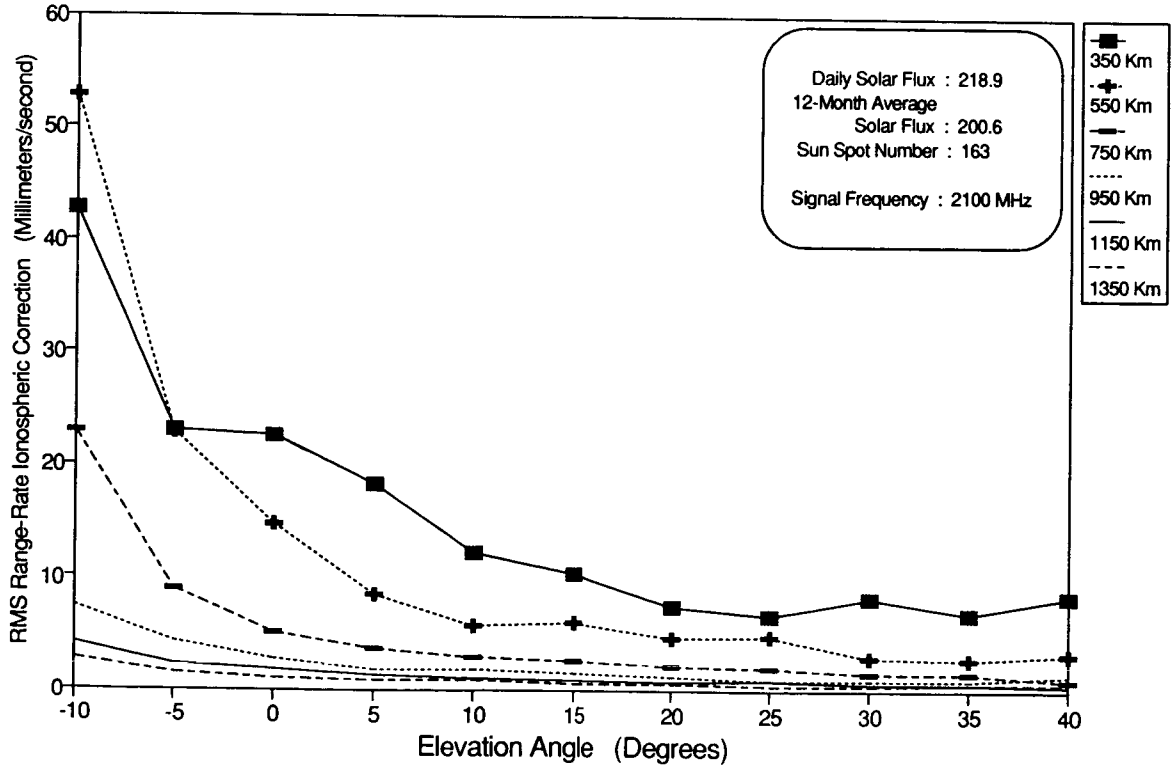

Figure 5b. RMS Range-Rate Ionospheric Correction Versus Elevation Angle for a 99.03-Degree Inclination for Various Altitudes

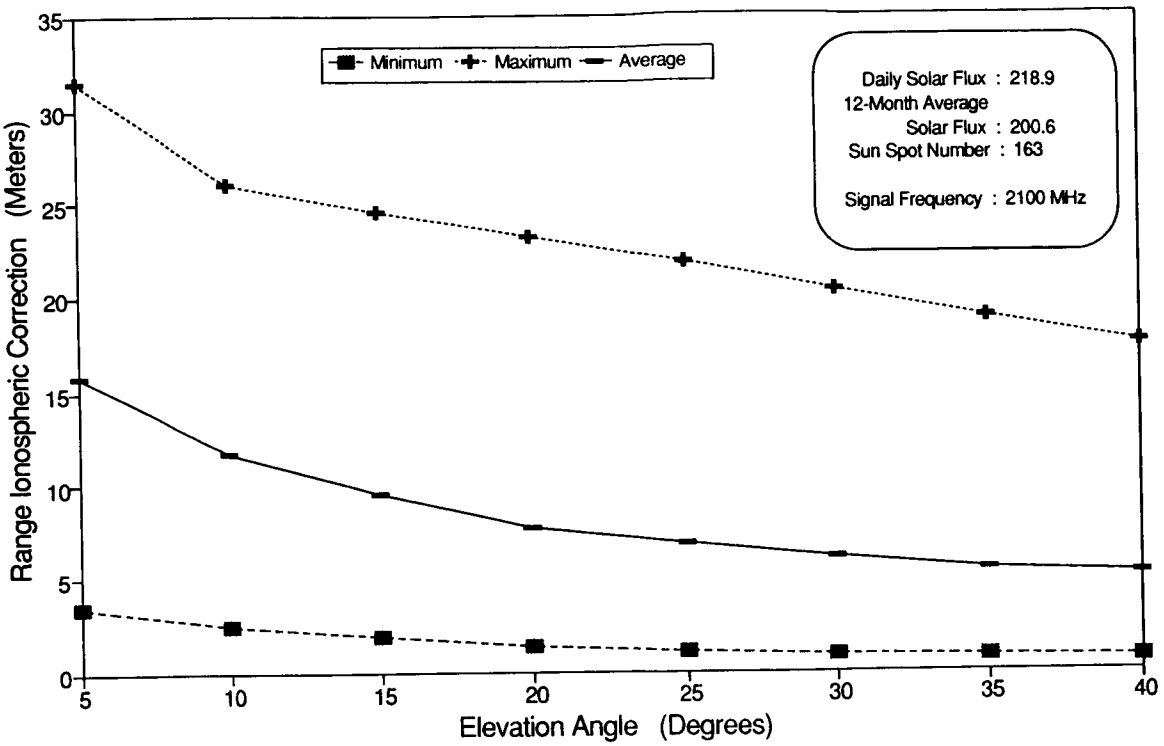

Figure 6a. Minimum, Maximum, and Average Range Ionospheric Correction Versus Elevation Angle for a 28.5-Degree Inclination and a 350-Kilometer Altitude

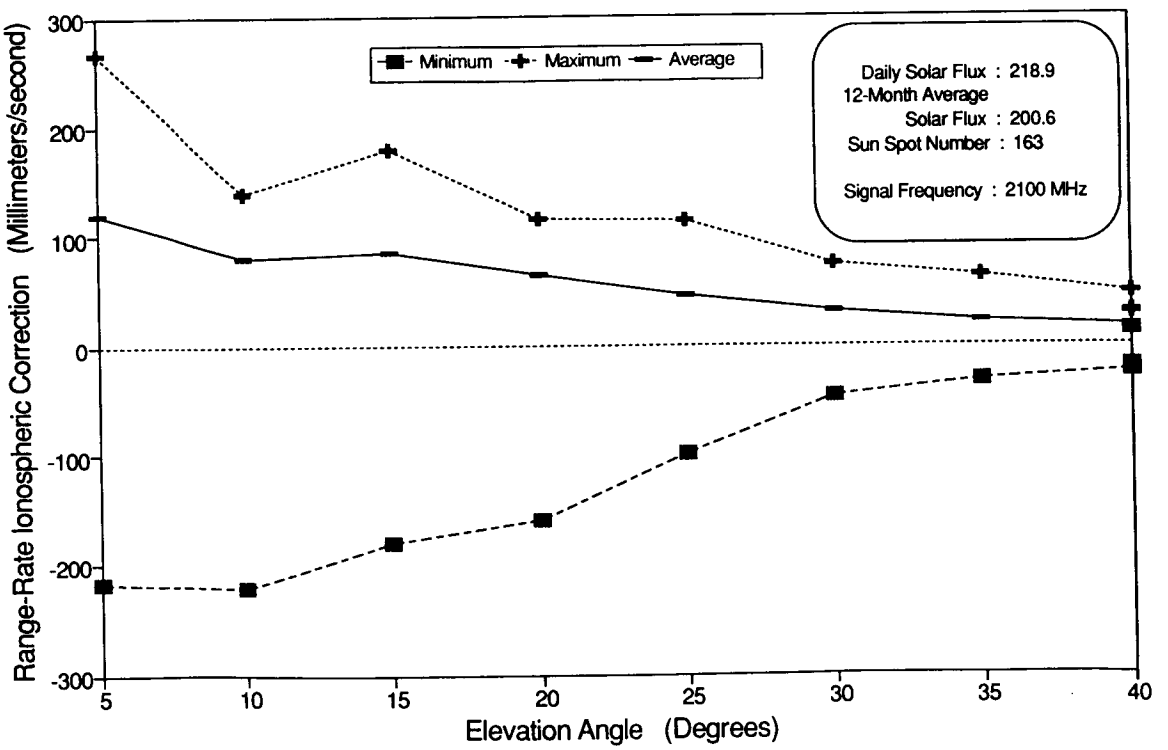

Figure 6b. Minimum, Maximum, and RMS Range-Rate Ionospheric Correction Versus Elevation Angle for a 28.5-Degree Inclination and a 350-Kilometer Altitude

As noted earlier, the upper bound of the ionosphere was set at 3000 kilometers. This choice is somewhat arbitrary. Although the contributions from altitudes above 3000 kilometers are not included in the results presented in this paper, their magnitudes can be estimated by evaluating the integral of Equation (3) all the way to the TDRS altitude. Analyzing these magnitudes obtained for a few sample tracking passes, it was found that they could vary significantly according to the altitudes of the user spacecraft. For a spacecraft at an altitude of 350 kilometers, for example, the contribution from above 3000 kilometers to the measurement correction was, in general, less than 5 percent of the contribution from below 3000 kilometers. However, for a spacecraft at 1350 kilometers, the contribution from above 3000 kilometers was found to be as high as 40 percent of the contribution from below 3000 kilometers.

2.1.2 Local Solar Times of Measurement

The ionospheric electron density for any location over the Earth's surface is also a function of the local solar time. This effect has been incorporated in the Bent electron density model. Because of this functional dependence, it is conceivable that the ionospheric refraction corrections for a particular range or range-rate measurement can be dependent on the local solar times of the relay and user spacecraft. For the spacecraft orbits studied, the ionospheric refraction correction was found to be affected more significantly by the local times of user spacecraft, with maximum corrections occurring around local times of 12 to 16 hours. This effect was consistently observed for all the spacecraft orbits studied.

Figure 7 shows the average range ionospheric refraction corrections as a function of the local solar time of the user spacecraft at the time of measurement. The spacecraft orbits shown are at three different orbital inclinations—28.5, 63.14, and 99.03 degrees—at a fixed altitude of 350 kilometers. This figure indicates a big increase in ionospheric refraction correction values around the user spacecraft local times of 12 to 16 hours, peaking at approximately 15 hours. The same trend was also observed for RMS range-rate corrections.

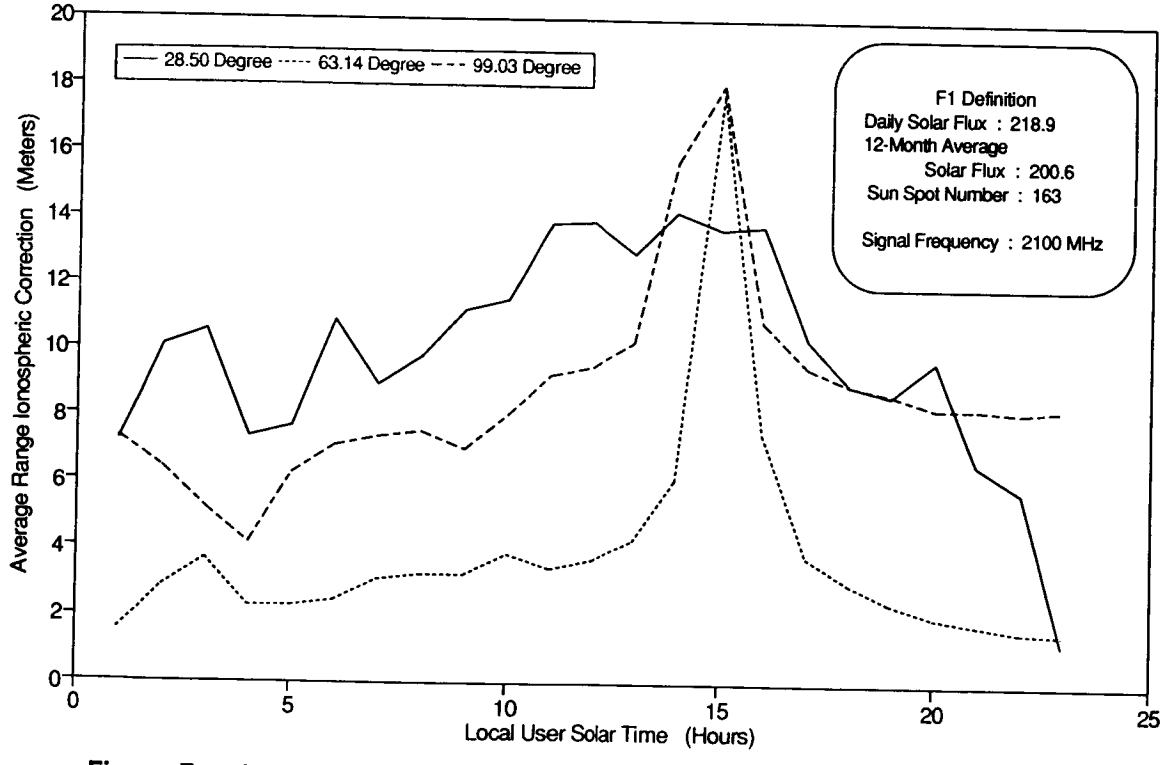

Figure 7. Average Range Ionospheric Correction Versus Local User Solar Time for a 350-Kilometer Altitude and Various Inclinations

If this phenomenon manifested by the Bent model closely matches the real ionospheric behavior, this may suggest that to effectively exclude the tracking data subject to high ionospheric disturbance, it might also be necessary to take into account the local time of the user spacecraft as a data editing criterion, together with the

tracking geometry considerations. A data editing criterion based on tracking geometry characterized by the height of ray path and the central angle is presently employed in the operational GTDS. In this practice, tracking data obtained at a height of ray path below a certain prescribed value and a central angle greater than a certain prescribed value are excluded. The prescribed values used are specific to mission requirements.

2.1.3 Solar Activity

To study the effects of solar activity on the ionospheric refraction correction, three sets of solar data were used, as summarized in Table 1. F1, F2, and F3 represent cases of moderately high, medium, and low solar activities, respectively.

Table 1. Solar Data Used for Ionospheric Refraction Simulations

SIMULATION NUMBER	DAILY SOLAR FLUX*	12-MONTH AVERAGE SOLAR FLUX*	SUN SPOT NUMBER
F1	218.9	200.6	163
F2	159.2	111.4	56
F3	74.4	76.1	20

* UNITS = 10^{-22} WATTS/METER^2/HERTZ

Figures 8 and 9 illustrate the average ionospheric refraction correction of range data as a function of elevation angle and solar activity for 350-kilometer and 1350-kilometer altitudes, respectively, at a 63.14-degree inclination. It can be seen that the ionospheric refraction correction values increase as the solar activity increases. For range corrections as shown in Figure 8, the values for the F1 curve are about two times higher than the corresponding F2 curve, and F2 is about two times larger than the corresponding F3 curve. Similar trends were also observed for RMS range-rate corrections.

To study the sensitivity of ionospheric refraction corrections to the daily and 12-month average or mean solar flux values, range corrections for two tracking passes, one for a 350-kilometer orbit and one for a 1350-kilometer orbit, were computed using different daily and mean solar flux values. The daily and mean solar flux values were varied in steps of 50 units. Whenever the mean solar flux was changed, the corresponding sunspot number was also changed according to an empirical formula that relates the sunspot number to the mean solar flux (Reference 3).

The results are summarized in Table 2. The values in cases 1, 3, and 5 were obtained using a common daily solar flux level of 218.9 with different mean solar flux levels. The values in cases 2, 3, and 4 were obtained with the same mean solar flux level of 200.6 and different daily solar flux levels. These results indicate that, in general, the refraction correction depends more strongly on the mean solar flux than on the daily flux. This general trend, however, does not appear to hold for the part of a pass with lower elevation angles.

2.1.4 Orbital Inclination

From Figures 3 through 5, it can be determined that the average or RMS values of ionospheric refraction obtained at various elevation angles for low-inclination (28.5-degree) orbits tend to be higher than those of high-inclination (99.03-degree) orbits. This tendency is found to be more pronounced in the low-altitude region (350 kilometers). At the 1350-kilometer altitude, the ionospheric refraction corrections for all three orbital inclinations are in the same neighborhood.

The observed dependence of the measurement refraction corrections on orbital inclination could be, at least partially, due to the strong dependence of the maximum electron density (N_m) and the corresponding height (h_m) on the latitude. Table 3 presents the values of these two parameters as a function of latitude. These results were obtained using the Bent model at a longitude of 318 degrees and a local solar time of 15 hours.

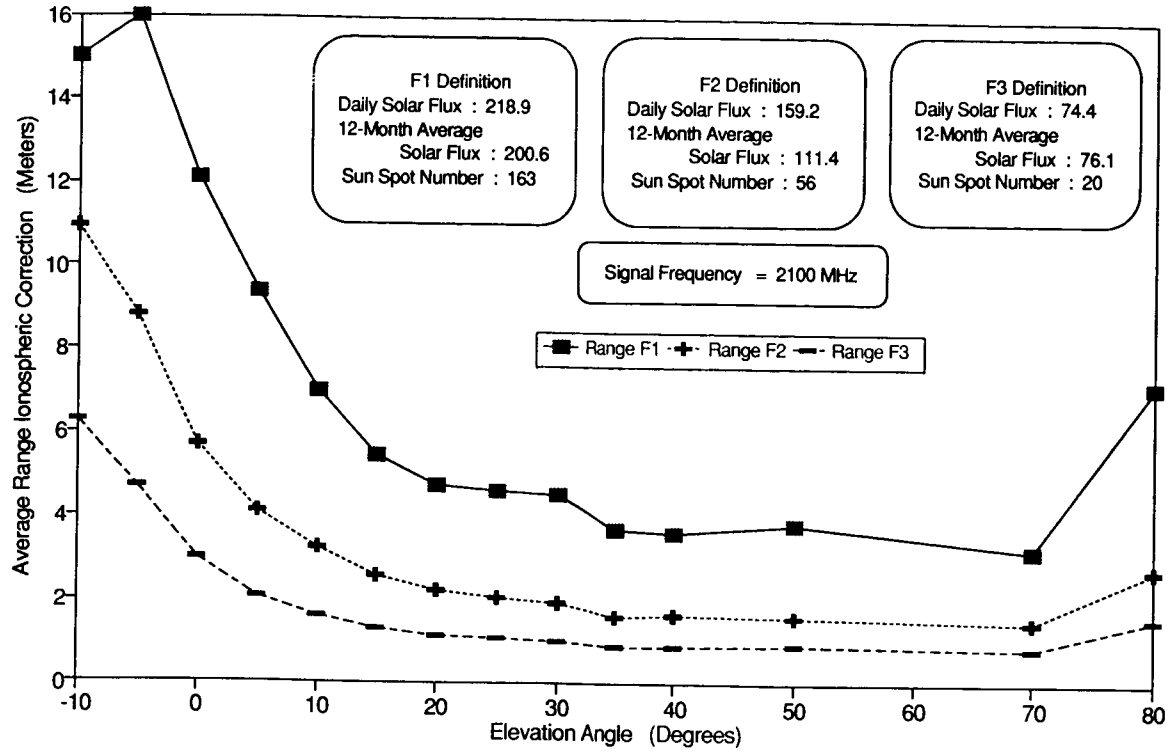

Figure 8. Average Range Ionospheric Correction Versus Elevation Angle for a 63.14-Degree Inclination, a 350-Kilometer Altitude, and Various Flux Levels

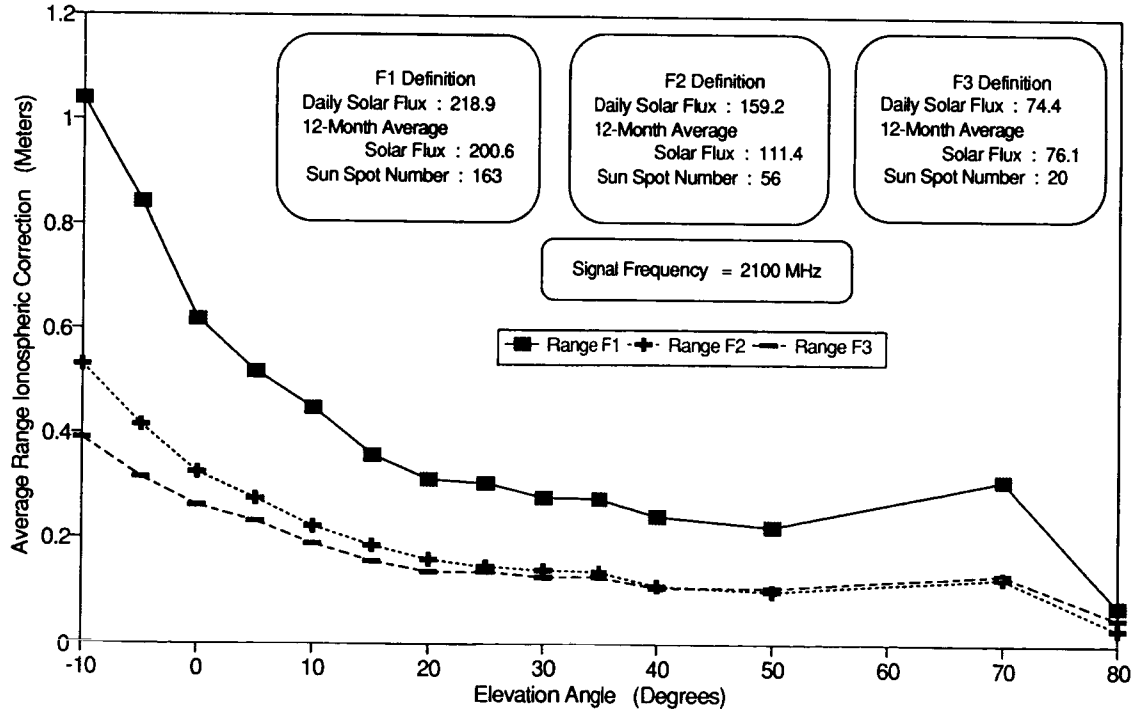

Figure 9. Average Range Ionospheric Correction Versus Elevation Angle for a 63.14-Degree Inclination, a 1350-Kilometer Altitude, and Various Flux Levels

Table 2. Daily and Mean Solar Flux Dependence of Ionospheric Refraction Corrections for Range Measurements

EPOCH: FEBRUARY 1, 1990; $0^h0^m0^s$
ORBIT: 350-KILOMETER ALTITUDE; 28.5-DEGREE INCLINATION

TIME (MINUTES FROM EPOCH)	ELEVATION ANGLE (DEGREES)	RANGE CORRECTIONS (METERS)				
		CASE 1	CASE 2	CASE 3	CASE 4	CASE 5
5	7.6	15.15	20.23	24.05	28.23	24.42
10	24.6	2.35	3.64	4.20	4.87	5.76
15	41.4	1.08	1.61	1.79	1.97	2.52
20	55.6	0.80	1.14	1.26	1.39	1.73
25	61.3	0.74	1.02	1.13	1.25	1.55
30	53.7	1.22	1.70	1.96	2.20	2.77
35	38.8	2.00	2.92	3.58	4.34	5.12
40	22.0	1.58	2.14	2.47	2.74	3.11
45	5.0	5.10	7.04	8.13	9.35	10.01
DAILY SOLAR FLUX*		218.9	168.9	218.9	268.9	218.9
12-MONTH MEAN SOLAR FLUX*		150.6	200.6	200.6	200.6	250.6

EPOCH: FEBRUARY 1, 1990; $0^h0^m0^s$
ORBIT: 1350-KILOMETER ALTITUDE; 28.5-DEGREE INCLINATION

TIME (MINUTES FROM EPOCH)	ELEVATION ANGLE (DEGREES)	RANGE CORRECTIONS (METERS)				
		CASE 1	CASE 2	CASE 3	CASE 4	CASE 5
5	2.6	0.61	0.89	1.09	1.33	1.51
10	16.4	0.18	0.26	0.29	0.34	0.39
15	30.1	0.10	0.13	0.13	0.14	0.17
20	43.3	0.07	0.09	0.09	0.09	0.11
25	54.6	0.07	0.08	0.08	0.08	0.09
30	60.5	0.07	0.08	0.08	0.09	0.09
35	57.4	0.08	0.09	0.09	0.10	0.11
40	47.4	0.10	0.12	0.14	0.17	0.21
45	34.6	0.12	0.14	0.15	0.18	0.19
50	20.9	0.15	0.18	0.19	0.19	0.21
DAILY SOLAR FLUX*		218.9	168.9	218.9	268.9	218.9
12-MONTH MEAN SOLAR FLUX*		150.6	200.6	200.6	200.6	250.6

*SOLAR FLUX UNITS = 10^{-22} WATTS/METER^2/HERTZ

As can be seen from this table, both h_m and N_m, especially the latter, increase in the lower latitude region. The parameter N_m acts as a scale factor for the entire electron density profile, thus affecting the electron densities computed in all different height regions. The variation of the maximum electron density height (h_m) can also contribute to an increase in the refraction corrections for orbits with lower inclinations. The values of N_m and h_m as a function of latitude were examined for several other longitudes, and all showed the trend similar to that described in Table 3.

Table 3. Latitude Variation of the Maximum Electron Density (N_m) and the Corresponding Height (h_m)

LATITUDE (DEGREES)	h_m (KILOMETERS)	N_m (10^{10} ELECTRONS/ METER^3)	LATITUDE (DEGREES)	h_m (KILOMETERS)	N_m (10^{10} ELECTRONS/ METER^3)
88.47	382.13	60.708906	-88.40	379.49	33.860825
82.38	363.65	49.976265	-78.17	361.63	45.700007
73.69	342.92	65.968391	-70.16	352.95	54.567174
61.99	325.73	118.187695	-59.07	346.42	79.233256
51.39	319.81	170.900019	-47.15	345.39	124.645481
44.31	320.52	192.604224	-38.04	349.87	164.401967
34.30	328.01	201.218013	-30.12	361.66	196.020009
21.03	352.92	213.455625	-18.44	409.45	215.195575
19.38	398.08	272.916559	-7.19	464.41	170.750405

NOTES: EPOCH = FEBRUARY 1, 1990
DAILY SOLAR FLUX = 218.9 (10^{-22} WATTS/METER^2/HERTZ)
12-MONTH MEAN SOLAR FLUX = 200.6 (10^{-22} WATTS/METER^2/HERTZ)
LONGITUDE = 318 DEGREES
LOCAL SOLAR TIME = 15^h

2.2 EFFECTS OF NEGLECTING SPACECRAFT-TO-SPACECRAFT IONOSPHERIC REFRACTION ON ORBIT DETERMINATION ACCURACY

As stated in Section 1, the current operational practice using GTDS ignores the ionospheric refraction effects for the spacecraft-to-spacecraft links of TDRSS measurements. It is therefore desirable to know for different types of spacecraft missions the magnitude and characteristics of the spacecraft orbit errors that can result by ignoring these effects. As the ionospheric refraction effect is functionally dependent upon various parameters that influence the electron density, a comprehensive study of this kind would require extensive investigations involving combinations of various mission scenarios and various parameters. This section presents the orbit determination error analysis results for the routine orbit determination scenario of a GRO-type spacecraft.

Because the primary interest of the study was the ionospheric refraction effects, the study was limited to investigating how ionospheric refraction of spacecraft-to-spacecraft links influences the orbit determination accuracy. A detailed orbit analysis investigation for the GRO spacecraft mission using ODEAS can be found in Reference 6.

2.2.1 Error Analysis Results

The GRO spacecraft is scheduled to be launched in late 1990. In this study, the nominal operational orbit of the GRO spacecraft was modeled as a near-circular orbit, with an orbital height of 350 kilometers and an inclination of 28.5 degrees. The orbital period for this orbit was 91.54 minutes. Routine orbit determination of the GRO spacecraft was simulated by processing 30-hour definitive data arcs in which the orbital state of the GRO spacecraft and the atmospheric drag scaling factor (ϱ_1) were simultaneously estimated together with the orbital elements of TDRS-East and TDRS-West. To see the effects of ionospheric refraction on the spacecraft orbit errors for different tracking geometries and tracking pass lengths, four tracking scenarios (T1 through T4) were simulated; the details of these scenarios are given in Table 4. All four tracking scenarios involved one TDRSS tracking pass per GRO revolution, alternating between TDRS-East and TDRS-West. For scenarios T1 and T2, tracking pass lengths were limited to 5 minutes each; whereas in scenarios T3 and T4, tracking pass lengths were limited to 20 minutes each. In scenarios T1 and T3, the tracking measurements are subject to relatively high ionospheric refraction effects; whereas in scenarios T2 and T4, the ionospheric refraction effects are relatively small.

Table 4. Simulated Tracking Scenarios for GRO Routine Orbit Determination

TRACKING* SCENARIO	RELAY SPACECRAFT	MINIMUM ELEVATION ANGLE (DEGREES)	MAXIMUM ELEVATION ANGLE (DEGREES)	AVERAGE ELEVATION ANGLE (DEGREES)	NUMBER OF MEASUREMENTS	IONOSPHERIC CORRECTIONS		
						AVERAGE RANGE (METERS)	RMS RANGE-RATE (MILLIMETERS/ SECOND)	AVERAGE RANGE-RATE (MILLIMETERS/ SECOND)
T1	TDRS-EAST	-12.9	7.53	-2.7	310 (RANGE) 310 (RANGE-RATE)	18.2	98.66	6.43
	TDRS-WEST	-13.3	10.5	-2.1	310 (RANGE) 310 (RANGE-RATE)	17.1	84.99	1.16
T2	TDRS-EAST	58.8	88.53	71.1	310 (RANGE) 310 (RANGE-RATE)	2.84	2.59	-0.94
	TDRS-WEST	43.5	84.6	63.8	310 (RANGE) 310 (RANGE-RATE)	4.14	7.15	0.99
T3	TDRS-EAST	-15.1	69.13	24.2	1210 (RANGE) 1210 (RANGE-RATE)	7.97	51.55	-0.07
	TDRS-WEST	-13.3	86.6	24.2	1210 (RANGE) 1210 (RANGE-RATE)	8.57	48.20	-0.79
T4	TDRS-EAST	33.2	88.53	60.4	1210 (RANGE) 1210 (RANGE-RATE)	3.05	3.95	-0.88
	TDRS-WEST	11.4	88.6	55.7	1210 (RANGE) 1210 (RANGE-RATE)	4.70	10.08	1.33

NOTES:
1. TDRSS TWO-WAY RANGE AND TWO-WAY RANGE RATE WITH TDRSS S-BAND SINGLE-ACCESS (SSA) SERVICE
2. 3σ RANGE NOISE = 1.5 METERS; WEIGHT = 90 METERS
   3σ RANGE-RATE NOISE = 0.004 METER/SECOND; WEIGHT = 0.1 METER/SECOND
3. DATA RATE = ONE RANGE AND ONE RANGE-RATE MEASUREMENT EVERY 10 SECONDS

* T1 AND T2 = 5-MINUTE TRACKING PASS PER GRO REVOLUTION, ALTERNATING BETWEEN TDRS-EAST AND TDRS-WEST
T3 AND T4 = 20-MINUTE TRACKING PASS PER GRO REVOLUTION, ALTERNATING BETWEEN TDRS-EAST AND TDRS-WEST

For each of the error analysis simulations, the ionospheric refraction corrections for TDRS-East-to-GRO and TDRS-West-to-GRO tracking links were included as considered error sources, with their respective 3σ errors set to be 100 percent of the spacecraft-to-spacecraft ionospheric refraction correction. Error analysis results obtained for the four tracking scenarios are summarized in Table 5. The contribution from the range and range-rate measurements are given separately for spacecraft-to-spacecraft tracking involving the TDRS-East and TDRS-West relay spacecraft. Total contributions from the range and range-rate measurements listed in the table are obtained by treating these quantities as fully correlated parameters. The maximum position errors listed are the maximum errors encountered during the 30-hour data arc for each position component error, which may not necessarily occur at the same time.

Error analysis results for scenarios T1 and T2 show that the GRO spacecraft position errors contributed by spacecraft-to-spacecraft ionospheric refraction can vary significantly, depending on the geometry of the tracking measurements included in the orbit estimation process. As shown in Table 4, the number of tracking passes and measurements included in T1 and T2 are the same, except that the measurements included in T1 have substantially lower elevation angles than those of T2 and are therefore subject to higher ionospheric disturbance than T2. Because of this, the GRO spacecraft position errors contributed by the spacecraft-to-spacecraft ionospheric refraction are found to be substantially higher in T1 than in T2, as shown in Table 5. In scenario T1, the maximum root-sum-square (RSS) position errors contributed by the TDRS-East and TDRS-West tracking measurements are 57.82 and 91.90 meters respectively; whereas in scenario T2, the same position error contributions are only 3.78 and 9.76 meters, respectively. The results suggest that by properly selecting the tracking measurements with favorable tracking geometries, the maximum RSS position errors can be reduced by as much as 50 to 80 meters. The same trend can be observed by comparison of scenarios T3 and T4.

Comparison of scenarios T1 with T3 and T2 with T4 also show the effects of tracking pass lengths on the spacecraft position errors. In the tracking scenarios studied, the spacecraft-to-spacecraft ionospheric refraction effects on the GRO spacecraft position errors are found to be generally smaller for longer tracking pass lengths. It should be noted that in all the simulated cases, the tracking scenarios associated with the longer tracking pass lengths also have better tracking geometries. Therefore, the effects observed in the above scenarios may be due to the combined effect of longer tracking pass lengths and better geometries.

To illustrate the relationship between the ionospheric refraction correction versus the resulting spacecraft position errors, Table 6 lists the ionospheric refraction corrections and the corresponding maximum RSS position errors contributed separately from the range and range-rate measurements. A general trend can be observed from this table indicating that an increase in the average value (for range measurement) or the RMS value (for range-rate measurement) of ionospheric refraction correction results in an increase in the maximum RSS position errors. However, this general trend does not hold very well between scenarios T4 and T2, where the magnitudes of corrections are small.

3.0 CONCLUSIONS AND RECOMMENDATIONS

The magnitudes of ionospheric refraction correction for spacecraft-to-spacecraft tracking links can vary depending upon the various parameters that affect the electron densities. The parameters studied include the local solar times of the measurements; solar activity; spacecraft inclination; and the tracking geometry, which is characterized by (1) the elevation angle of the TDRS with respect to the TDRS user spacecraft and (2) the orbital height. The following general conclusions can be made regarding the spacecraft-to-spacecraft ionospheric refraction:

- The ionospheric refraction corrections for both range and range-rate measurements increase with the decrease in the elevation angle of the TDRS with respect to the TDRS user spacecraft. This suggests that to avoid high ionospheric disturbance in tracking data, data taken at very low elevation angles should be excluded. For high spacecraft altitudes (950 kilometers and up), the magnitudes of ionospheric corrections are much smaller than those for the lower altitudes, but the overall trend of elevation angle dependence still exists.

- The ionospheric refraction correction is found to be a strong function of the local solar time of the TDRS user spacecraft at the time of measurement. It was found that measurements taken between 12 to

Table 5. GRO Spacecraft Position Errors Contributed by Spacecraft-to-Spacecraft Ionospheric Refraction Effects for Different Simulated Tracking Scenarios

TRACKING* SCENARIO	IONOSPHERIC REFRACTION ERROR SOURCE		POSITION ERROR AT EPOCH (METERS)				POSITION ERROR AT END OF DATA (METERS)				MAXIMUM POSITION ERROR COMPONENT (METERS)			
	SPACECRAFT	MEASUREMENT TYPE	HEIGHT	CROSS-TRACK	ALONG-TRACK	RSS	HEIGHT	CROSS-TRACK	ALONG-TRACK	RSS	HEIGHT	CROSS-TRACK	ALONG-TRACK	RSS
T1	TDRS-EAST	RANGE	1.10	1.01	18.2	18.2	−0.863	−0.863	11.4	11.5	−1.10	1.27	18.19	18.25
		RANGE-RATE	−8.95	−26.6	−48.2	55.8	11.9	−41.6	−28.0	51.5	−12.94	−47.63	−53.28	60.09
		TOTAL	−7.86	−27.6	−30.0	41.6	11.5	−42.5	−16.6	47.0	12.93	−48.87	−49.69	57.82
	TDRS-WEST	RANGE	−1.74	−2.06	−14.4	14.6	1.493	0.461	−17.0	17.1	1.96	−2.08	17.00	17.07
		RANGE-RATE	12.5	−67.4	3.26	68.6	10.2	−9.11	75.6	76.8	20.03	−47.63	80.92	96.17
		TOTAL	10.7	−69.4	−11.2	71.1	11.7	−8.65	58.6	60.2	−19.63	−71.54	68.51	91.90
T2	TDRS-EAST	RANGE	0.189	−0.218	−0.097	0.304	−0.011	−1.01	0.441	1.10	0.198	1.06	0.443	1.147
		RANGE-RATE	0.495	2.01	0.011	2.07	0.22	−1.47	1.48	2.10	0.652	2.39	1.98	2.95
		TOTAL	0.685	1.79	−0.086	1.92	0.209	−2.48	1.92	3.14	0.826	−2.94	2.38	3.78
	TDRS-WEST	RANGE	0.410	−0.145	−0.165	0.465	−0.053	−1.50	1.16	1.90	0.419	−1.54	1.16	1.899
		RANGE-RATE	1.39	2.64	−5.80	6.52	−0.056	−2.93	4.87	5.69	−1.565	−3.77	−7.75	8.386
		TOTAL	1.80	2.49	−5.97	6.71	−0.109	−4.43	6.03	7.49	−1.971	−4.91	−8.57	9.76
T3	TDRS-EAST	RANGE	0.626	−0.626	3.61	3.72	0.119	−0.741	4.04	4.11	0.766	−1.036	4.993	5.008
		RANGE-RATE	−3.18	−0.057	−18.0	18.3	5.55	−15.9	−7.35	18.4	−5.681	16.058	−18.236	21.925
		TOTAL	−2.55	−0.683	−14.4	14.6	5.43	−16.64	−3.31	17.81	−5.72	−16.90	−14.66	20.13
	TDRS-WEST	RANGE	−0.448	−2.48	−4.46	5.12	0.930	−0.320	−3.01	3.17	0.930	−2.555	−4.456	5.118
		RANGE-RATE	0.660	−9.29	−4.97	10.6	4.136	−16.5	9.65	19.6	4.835	20.069	14.287	21.637
		TOTAL	0.212	−11.77	−9.43	15.08	5.06	−16.82	6.64	18.78	5.52	−3.86	13.27	23.18
T4	TDRS-EAST	RANGE	0.181	−0.191	−0.072	0.272	−0 .0302	−0.965	0.404	1.05	0.183	−1.014	0.404	1.084
		RANGE-RATE	−0.237	2.12	−0.536	2.20	0.278	−1.76	0.622	1.89	0.4497	2.648	1.063	2.795
		TOTAL	0.418	1.93	−0.607	2.07	0.248	−2.73	1.026	2.92	0.589	−3.212	1.327	3.48
	TDRS-WEST	RANGE	0.466	−0.0007	0.030	0.467	−0.133	−1.34	1.28	1.85	0.466	1.349	1.278	1.855
		RANGE-RATE	0.682	2.21	−2.90	3.71	0.103	−5.31	−0.418	5.32	−0.823	5.596	−3.704	6.623
		TOTAL	1.15	2.21	−2.87	3.80	−0.030	−6.65	0.862	6.71	−1.252	6.859	04.537	8.185

* T1 AND T2 = 5-MINUTE TRACKING PASS PER GRO REVOLUTION, ALTERNATING BETWEEN TDRS-EAST AND TDRS-WEST
T3 AND T4 = 20-MINUTE TRACKING PASS PER GRO REVOLUTION, ALTERNATING BETWEEN TDRS-EAST AND TDRS-WEST

Table 6. Relationship Between the Spacecraft-to-Spacecraft Ionospheric Refraction Corrections Versus the Corresponding GRO Spacecraft Position Errors

TRACKING* SCENARIO	RELAY SPACECRAFT	AVERAGE IONOSPHERIC CORRECTION RANGE (METERS)	MAXIMUM POSITION ERROR DUE TO RANGE (METERS)	RMS IONOSPHERIC CORRECTION RANGE RATE (MILLIMETERS/ SECOND)	MAXIMUM POSITION ERROR DUE TO RANGE RATE (METERS)
T1	TDRS-EAST	18.2	18.25	98.66	60.09
T3	TDRS-EAST	7.97	5.01	51.55	21.93
T4	TDRS-EAST	3.05	1.08	3.95	2.80
T2	TDRS-EAST	2.84	1.15	2.59	2.95
T1	TDRS-WEST	17.1	17.07	84.99	96.17
T3	TDRS-WEST	8.57	5.12	48.20	21.64
T4	TDRS-WEST	4.70	1.86	10.08	6.62
T2	TDRS-WEST	4.14	1.90	7.15	8.39

* T1 AND T2 = 5-MINUTE TRACKING PASS PER GRO REVOLUTION, ALTERNATING BETWEEN TDRS-EAST AND TDRS-WEST
T3 AND T4 = 20-MINUTE TRACKING PASS PER GRO REVOLUTION, ALTERNATING BETWEEN TDRS-EAST AND TDRS-WEST

16 hours of local solar time tend to have significantly higher ionospheric disturbance than those taken at different local solar times. If this phenomenon manifested by the Bent model closely matches the real ionospheric behavior, this may suggest a need to take into account the local time of the user spacecraft as a data editing criterion, together with the tracking geometry considerations, to effectively exclude the tracking data subject to high ionospheric disturbance. A data editing criterion based on tracking geometry, characterized by the height of the ray path and the central angle, is presently employed in the operational GTDS. To verify this local solar time effect, future studies should include assessing the orbit determination accuracy using real tracking data to determine whether more accurate spacecraft orbits can be realized by using a data editing criterion that excludes those tracking data taken at a user spacecraft local solar time around 15 hours and at very low elevation angles.

- The ionospheric refraction correction is found to be a strong function of solar activity. For a spacecraft orbit at a 350-kilometer altitude and 28.5-degree inclination, the ionospheric refraction correction values obtained at a moderately high solar activity [average solar flux = 200.6, daily solar flux = 218.9 (units = 10^{-22} watts/ meters^2/hertz)] can be twice as large as the corrections obtained at a relatively lower solar activity [average solar flux = 111.4, daily solar flux = 159.2 (units = 10^{-22} watts/ meters^2/hertz)]. It was also found that the ionospheric refraction effect is more sensitive to the 12-month average solar flux level than the daily solar flux level.

- The maximum electron density value, N_m, as defined on the Bent electron density profile, has a strong latitude dependence. It was found that N_m values tend to be higher in low latitude (near-equatorial) regions than in the high-latitude (polar) regions. It is therefore conceivable that in a particular spacecraft orbit, the ionospheric refraction effects may tend to be high if many of the tracking measurements were taken when the user spacecraft was near the equatorial region. This may explain why the ionospheric refraction corrections observed in the study tend to be generally higher for the low-inclination (28.5-degree) orbits than those of the high-inclination (99.03-degree) orbits.

From the error analysis results of the GRO spacecraft, the following conclusions can be drawn:

- The spacecraft position errors contributed by spacecraft-to-spacecraft ionospheric refraction can vary significantly, depending on the geometry of the tracking measurements included in the orbit estimation

process. In a routine orbit determination involving 30 hours of data with 5 minutes of TDRSS tracking per GRO revolution, selecting the tracking measurements with favorable tracking geometries can reduce the spacecraft maximum RSS position errors from 57.82 meters to 3.78 meters (in the case of TDRS-East-to-GRO ionospheric refraction contribution) and from 91.90 meters to 9.76 meters (in the case of TDRS-West-to-GRO ionospheric refraction contribution).

- An increase in the mean value of the ionospheric refraction correction is found to be associated with an increase in the maximum RSS position errors. However, this general trend does not hold very well where the magnitudes of the ionospheric refraction corrections are small or the geometric quality of the processed data is appreciably altered. This general relationship also implies that parameters affecting the mean ionospheric refraction values, such as solar activity, will also affect the corresponding spacecraft orbit errors in a similar fashion.

ACKNOWLEDGMENT

The authors wish to thank A. Schanzle (Computer Sciences Corporation) for his thoughtful comments and M. Radomski (Computer Sciences Corporation) for providing reference materials and some useful discussions during preparation of this paper.

REFERENCES

1. Goddard Space Flight Center, Flight Dynamics Division, FDD/552-89/001, *Goddard Trajectory Determination System (GTDS) Mathematical Theory, Revision 1*, A. C. Long, J. O. Cappellari, Jr., C. E. Velez, and A. J. Fuchs (editors), July 1989

2. Bent, R. B., Llewellyn, S. K., Nesterczuk, G., Schmid, P. E., "The Development of a Highly Successful Worldwide Empirical Ionospheric Model and Its Use in Certain Aspects of Space Communication and Worldwide Total Electron Content Investigations," *Proceedings of the Ionospheric Effects Symposium*, Arlington, Virginia, January 20-22, 1975

3. Computer Sciences Corporation, CSC/TM-89/6037, *TDRSS User Orbit Determination Error Due to Ionospheric Refraction*, M. Radomski and A. Binebrink, September 1989

4. Goddard Space Flight Center, X-591-73-281, *NASA-GSFC Ionospheric Corrections to Satellite Tracking Data*, P. E. Schmid, R. B. Bent, S. K. Llewellyn, G. Nesterczuk, and S. R. Rangaswamy, December 1973

5. Goddard Space Flight Center, Flight Dynamics Division, FDD/554-90/029, *Orbit Determination Error Analysis System (ODEAS) Mathematical Specifications, Revision 1*, C. P. Yee and T. Lee, January 1990

6. Goddard Space Flight Center, Flight Dynamics Division, FDD/554-90/013, *Gamma Ray Observatory (GRO), 1990 Flight Dynamics Analysis Report 6, Orbit Determination Analysis*, J. Dunham, February 1990